16. H. Glunder, A. Gerhardt, H. Platzer, and J. Horter-Hiteis, "A Geometrical-Translation-Invariant Pattern Recognition Concept Incorporating Elementary Properties of Nercral Circuits," Proc. 7th Int. Conf. on Pattern Recognition, Vol. 2, Montreal, 1377-1379 (1984).

THERMAL CONDUCTIVITY OF LASER-PRODUCED PLASMA CORONA

N. G. Basov, P. P. Volosevich, E. G. Gamalii,
Yu. A. Zakharenkov, A. E. Kiselev, S. P. Kurdyumov,
E. I. Levanov, V. B. Rozanov, A. A. Rupasov,
A. A. Samarskii, G. V. Sklizkov, E. N. Sotskii,
and A. S. Shikanov

Various methods of theoretically describing the thermal conductivity of a of plasma corona are considered. The processes of laser heating and ablating a spherical-shell target in the "TRITON" program (Inst. of Appl. Mech., USSR Acad. Sci.) are computer-simulated. Numerical and analytic methods are used to investigate the influence of heat-transport suppression on the principal hydrodynamic characteristics of the plasma. It is shown that the most sensitive to a reduction of the heat transport is the electron-density distribution in space and in time. The requirements imposed on experimental measurements capable of determining, in comparison with numerical computations, the degree of heat-transport suppression, are analyzed for a large range of flux densities. It is shown that when the flux density is decreased to $\sim 10^{13}$ W/cm^2 the present accuracy of measuring the position of the critical-density region in the corona, as well as the rate of evaporation of the material, becomes inadequate to determine the deviation of the thermal conductivity from the classical value. Reliable conclusions concerning the transport coefficients can be drawn in this case from a comparison of high-speed interferometry data on the dynamics of a low-density corona ($\rho/\rho_{cr} = 10^{-3}$-10^{-1}) with the results of computer simulation.

1. INTRODUCTION

Electronic thermal conductivity is the main mechanism of energy transport from the laser-radiation absorption zone to the dense layers of the target in the case of laser heating and ablation of matter. In an equilibrium plasma (having a Maxwellian electron distribution) the electronic heat flux is well described by the Fourier law

$$\bar{q}_{cl} = -\varkappa_e T^{5/2} \mathbf{grad}(T) \qquad (1)$$

with the thermal conductivity coefficient calculated by Spitzer and Harn [1, 2].

It is shown in very many recent theoretical and experimental papers [3-9] that in many cases the electronic heat flux in a laser (and in an outer-space) plasma can be substantially lower than the classical value (1). In theoretical papers this decrease is attributed to spontaneous megagauss magnetic fields [10-12], to a lowering of the electron-collision frequency on account of developed ion-sound and other types of plasma turbulence [13-16], and also to the fact that the diffusion approximation, expressed by the condition ($\lambda_{ei} \ll L = T/|\mathrm{grad}(T)|$) is not valid [17-19].

The heat flux has an obvious physical upper bound – the flux cannot be higher than the free particle flow $q \approx n_e v_{te} T_e$ in vacuum (where n_e, v_{te} and T_e are the electron density,

---

Division of Quantum Physics, Lebedev Physics Institute, Academy of Sciences of the USSR.
Translated from Preprint No. 188 of the Lebedev Physics Institute, Academy of Sciences of the USSR, Moscow (1988).

 0270-2010/89/1005-0438$12.50

velocity, and temperature). In a phenomenological description of a heat flux smaller than classical, one therefore uses frequently in the calculations the simplest form of the so-called "limiting" flux

$$\bar{q}_{lim} = -fn_e v_{Te} T_e \frac{\nabla T_e}{|\nabla T_e|}, \tag{2}$$

where f is a constant determined by comparing the calculations with experiment. In most programs intended for the solution of high-temperature-plasma problems the use of the upper bound (2) for the flux reduces [20-22] to the use of interpolation equations of type

$$q = \min(q_{cl}, q_{lim}) \tag{3}$$

or

$$q^{-1} = q_{cl}^{-1} + q_{lim}^{-1} \tag{4}$$

Another rough phenomenological form of decreased heat flux is also used, in which the diffuse character of the transport is retained, but the coefficient of the electronic heat capacity in the region between the radiation-absorption region (the critical surface R_{cr}) and the ablation surface R_a is decreased by several times compared with the classical value [23]

$$\bar{q} = \begin{cases} a\bar{q}_{cl}, & R \in [R_1, R_2],\ a<1 \\ \bar{q}_{cl}, & R \notin [R_1, R_2] \end{cases} \tag{5}$$

where $R_{1,2}$ are the radii bounding the regions with the lower coefficient in the Fourier law.

In most experiments in which lasers are used to heat a substance one measures (in a single experiment) quantities such as the absorbed energy, the position of the region with the critical density ($n_{cr} = m_e w^2/4\pi e^2$) as a function of time, the average evaporation rate $dM/dt = \dot{M}$ of the target mass, the radial distribution of the electron density at various instants of time, the total plasma radiation and its spectrum, and a few others. It must be noted that if only the parameter f or a is varied it is impossible as a rule to obtain full agreement between the calculations and the entire aggregate of experimental data.

Comparison of the various experiments and calculations shows that the parameter f varies in range $0.01 \leq f \leq 0.6$, depending on the laser flux acting on the target. Analysis of a large body of experiments performed in [24] seems to offer evidence that a transition from classical flux to a reduced one with f = 0.01-0.03 takes place at fluxes $q_{las} = 10^{13}$-10^{14} W/cm^2.

Since a large fraction of the experiments with the "KAL'MAR" and "DEL'FIN" facilities [25-26] was performed at the Lebedev Physics Institute precisely in the above range of fluxes, it is of interest to compare these experiments with calculations, so as to determine the thermal conductivity (the value of f is models (2), (4) are used, or the value of a if expres-(5) is used). The purpose of the present paper is indeed such comparison with experiments on the "KAL'MAR" facility.

2. DESCRIPTION OF "TRITON" PROGRAM

Laser-beam activated heating, compression, and expansion processes were numerically simulated with the aid of the "TRITON" program [27], in which was realized a fully conservative difference scheme corresponding to the system of equations of one-dimensional two-temperature gasdynamics in Lagrangian mass coordinates. The "TRITON" program is a variant of the "DIANA" program [28], which makes it possible to take into account, beside the capabilities of the basic variant of the "DIANA" program, also the interaction of the plasma's own radiation with matter, phenomena that limit the heat fluxes, as well as the possible mass sources and sinks. The electronic thermal conductivity can be described in the "TRITON"

program by using the mathematical models (4) and (5), as well as some others [29]. In all the calculations, the influence of epithermal electrons was neglected, since the contribution of the resonance absorption to the total absorption is small at fluxes $< 10^{14}$ W/cm^2.

The properties of the thermal wave are not measured directly in the experiment. The heat flux is assessed from indirect data. Best agreement with the measured plasma characteristics is achieved by varying the parameter f (or a) in the numerical computation. When the "TRITON" program is used to determine the degree of suppression of the thermal conductivity, the following must be done to allow in the experiment for two circumstances:

1. Determine, by a set of preliminary calculations, which of the measured plasma parameters are most sensitive to a lowering of the thermal conductivity in the corona. It is just these values that must be used to obtain reliable information on the degree of suppression of the electronic thermal conductivity in a real physical experiment.

2. In programs used to solve laser-driven thermonuclear fusion ("LASNEX" [21], "TRITON." and others) the details of the physical model, the difference schemes, and their programming are all different. It is therefore advisable to compare the results of numerical simulation of one and the same physical experiment by using different programs.

3. CORONA HYDRODYNAMICS FOR $q_{las} > 10^{14}$ W/cm^2

To analyze the results of a numerical simulation of an experiment at a laser-emission flux density $q_{las} = 10^{14}$-10^{15} W/cm^2 we used data in [30, 31], which were used for computation by the "LASNEX" program.

The experimental data [30, 31] include the profiles of the electron-density profiles in the corona at various instants of time, the location of the critical-density region as a function of time, and the rate of matter evaporation $\dot{M}$ (at an absorbed energy ranging from 25 to 50 J).

"LASNEX" calculations [31] indicate that to reconcile the theoretical and experimental values it is necessary to limit the fluxes of both Maxwellian electrons and epithermal electrons with $f \approx 0.03$.

In analogy with [31], the "TRITON" program was used to calculate the contraction of the target (see Fig. 1) at absorbed energy values 25 and 50 J. In contrast to [31], in the "TRITON" program two computation runs were made for different descriptions of the electronic heat conduction, using mathematical models based on Eqs. (4) and (5). The constants f and a were varied in wide ranges ($0.03 < f < 0.6$, $0.03 < a < 1$).

Comparisons of the results of the numerical calculations with the experimental data of [31] are shown in Figs. 2 and 3, which show the time dependence of the position of the critical surface and the radial distribution of the electron density at various instants of time. It is seen from the figures that calculated experimental data do not agree if the electronic heat conduction is described classically. Agreement is achieved by limiting the heat flux in accordance with Eq. (4), with a parameter $f = 0.3$ in the expression (2) for the flux limit (this agrees with the conclusions of [31]), or by lowering the thermal conductivity more than tenfold ($a < 0.1$) when using Eq. (5).

Let us analyze the results.

We note first that the distance between the ablation and the critical surfaces in the corona depends substantially on f (or a). For any fixed instant of time a decrease of f (or a) decreases the value of $R_{cr}(t)$, see Figs. 2 and 4.

From an analysis of the stationary model of a corona with the flux given by (5) [23] it follows that there exists a certain critical value $a = a^*$ that satisfies the equation

$$a^* + 0.2 = 0.15\,\gamma_0 a^{*7/4} \qquad (6)$$

where $\gamma_0 = \frac{Q_0 \varkappa_c^{3/4}}{\rho_{cr}^{7/4} R_a^{11/4}} \left(\frac{M_i}{Z+1}\right)^{21/8}$, $[Q_0]$ is in W/cm^2·sr, M_i and Z are the average mass and ion charge, and $\varkappa_c$ is the coefficient in the Fourier law (1). This value of a^* characterizes the transi-

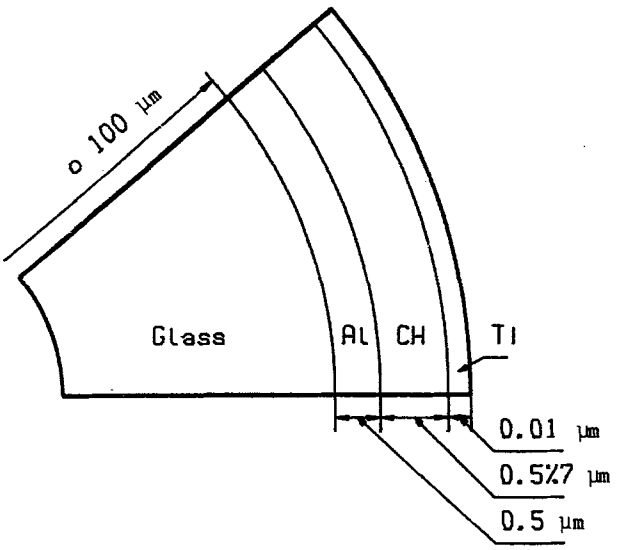

Fig. 1. Target scheme used in experiments [30] and [31]. The characteristic layer thicknesses and the chemical compositions are indicated in the figure.

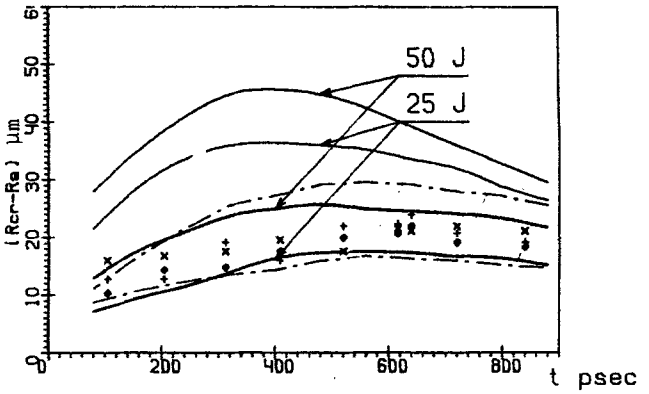

Fig. 2. Time dependence of the shift ($R_{cr} - R_a$) of the position of the critical surface relative to the initial target radius. Results of experiments of [31] – dashed band. Results of calculations by "TRITON" program: the solid thin lines bound the (R_{cr}–R_a) region obtained by varying the absorbed energy from 25 to 50 J for a classical heat-conduction law; solid thick lines – the same but for strong suppression of the heat conduction ($f \sim 0.03$, $a < 0.1$); – the symbols mark the values of ($R_{cr} - R_a$) obtained in three actual computations: ♦) model (5), $a = 0.03$; ×) model (5), $a = 0.1$; +) model (4), $f = 0.03$. The absorbed energy in these calculations is equal to 25 J.

tion that takes place when a from the continuous solutions of the stationary hydrodynamic equations is decreased ($a > a^*$) to solutions with discontinuities ($a < a^*$). For $a = a^*$ the radii R_{cr} and R_a of the critical and ablation surfaces are connected by the universal relation $R_{cr} = 1.2\ R_a$ [32], and the flow in the region with the critical density is acoustic.

Calculations show that the numerical value always remains continuous and, furthermore, the $R_{cr}(t)$ dependence becomes practically constant with decrease of $a < a^*$ (see Fig. 4). The average radius of the critical surface for $a \sim a^*$ is $R_{cr} \sim 1.2R_a$, which agrees with the results of the stationary corona model [23].

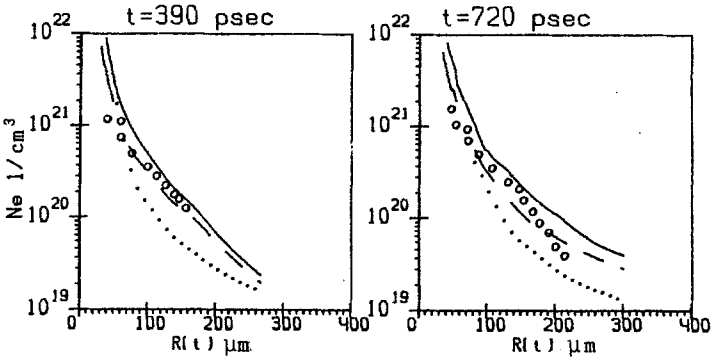

Fig. 3. Comparison of calculated and experimental dependences of the electron density on the radius at the instants of time 390 psec (left) and 720 psec (right): o) experimental data [31];) "TRITON" calculations, classical heat conduction;) model (4), f = 0.03;) model (5), a = 0.1.

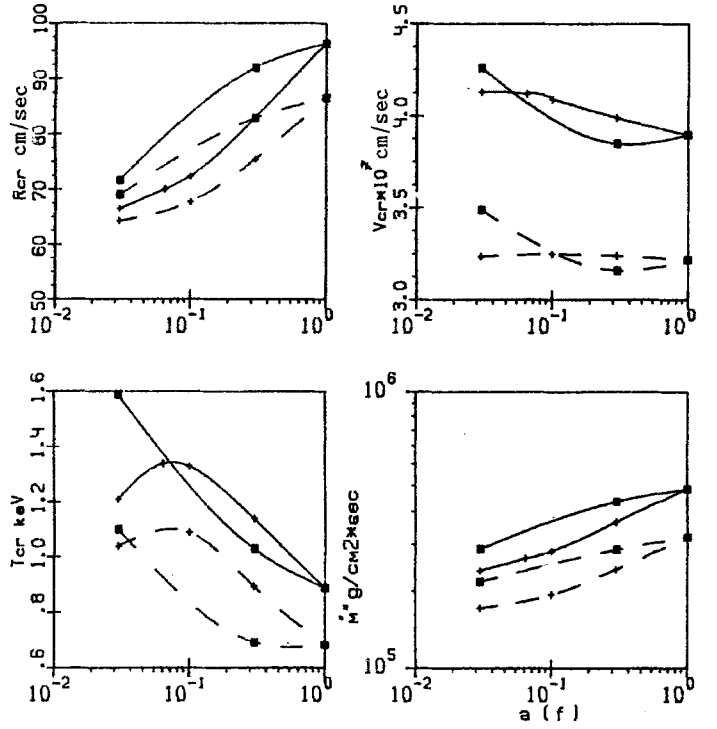

Fig. 4. Principal corona properties (critical radius R_{cr}, velocity v_{cr} of matter in the critical zone, electron temperature T_{cr} in initial zone, mass-evaporation rate $\dot{m}$) as functions of the degree of heat-transfer suppression. The values were taken for the instant of time 390 psec. The abscissas are f and a in logarithmic scale. Solid lines – results of calculations at an absorbed energy 50 J; dashed – 25 J. The symbols ▪ and + mark the results of calculations for models (4) and (5), respectively.

It is evident from Figs. 2 and 4 that R ceases to depend on the method used to describe the heat flow in the case of strong suppression of the heat transport ($f \sim 0.03$ or $a < a^* \sim 0.1$ for an absorbed laser energy 25 J and $f \sim 0.01$ or $a < a^* \sim 0.06$ for 50 J).

The heat-flow restriction of Eq. (4) influences almost the entire corona (where $q_{cl} > q_{lim}$). As a result, the corona as a whole moves more compactly. Suppression of heat transfer only in the zone between ablation and critical surfaces, in the form (5), leads first of all to a decrease of the size of this zone. The radial distribution of the density in the rarefied ($n_e < n_{cr}$) layers of the corona changes little with decrease of a (mainly because of the geometric connection with the critical surface $n_{cr}R^2 \sim n_eR^2$), see Fig. 3.

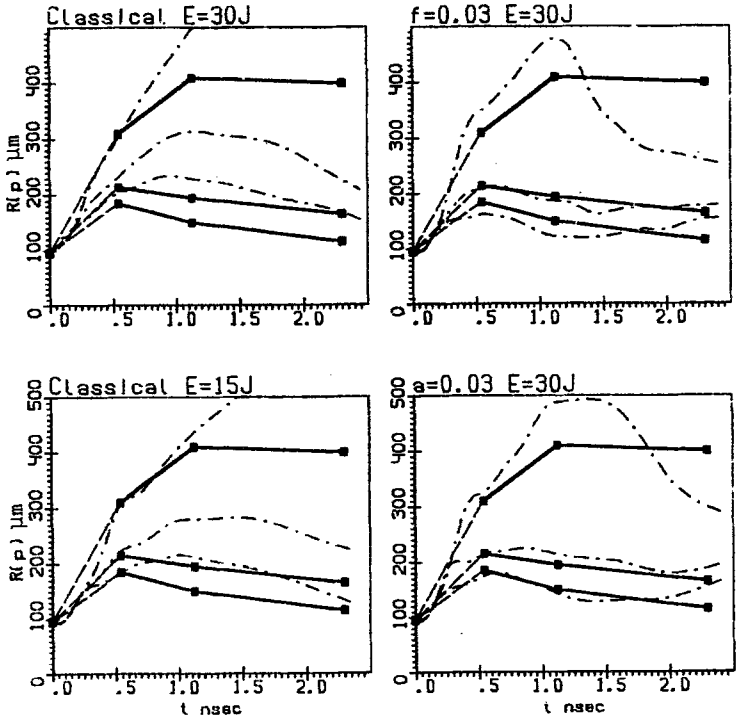

Fig. 5. Comparison of the experimental data ("KAL'MAR") with the calculated ("TRITON") R–t diagrams of the motion of the corona regions with specified values of electron density (n_e = 10^{19}, 5×10^{19}, and 10^{20} cm^{-3}). The calculations were performed at various values of absorbed energy using models (4) and (5) to describe the heat transfer. Solid lines) experiments, dash-dot) calculation results.

Comparison of the calculation data for other physical properties of the corona, such as the velocity v_{cr} of matter on the critical surface, the temperature T_{cr} of the critical-density zone, and the velocity $\dot{m} = \dot{M}/4\pi R_a^2$ of the target mass referred to the initial target surface area has shown that lowering the heat transfer (in both model (4) and model (5)) influences most strongly just the position of the critical surface (see Fig. 4).

Decreasing the absorbed energy from 50 to 25 J yields, for classical heat conduction, a much smaller change of the critical density than a decrease of f and a from 1 to 0.03. The remaining corona parameters (v_{cr}, T_{cr}, and $\dot{m}$) are approximately equally influenced by a twofold decrease of the absorbed energy or by a 30-fold suppression of the heat transfer.

Note that the dependences of all the physical properties of the corona R_{cr}, v_{cr}, T_{cr} and $\dot{m}$ on the degree of heat-transfer suppression in (5) turns out to be stronger at higher values of **a** (a > 0.3). This result is likewise in agreement with the concluions of [23]. In the inverse-flow model (4), on the contrary, the restriction of the heat flow comes substantially into play only if f is small enough (<0.1).

4. ANALYSIS OF THE EXPERIMENTAL ACCURACY

The "KAL'MAR" facility of the Lebedev Physics Institute was used to perform many experiments on the ablation of spherical glass targets [33] at laser fluxes $q_{las} < 10^{14}$ W/cm^2. In the course of these experiments, along with measuring the absorbed energy, interferometric measurements were made of the electron-density profiles $n_{cr}(R, t)$ with spatial and temporal resolution, the position of $R_{cr}(t)$ and of the point with density $n_{cr}/4$ ($R_{cr/4}(5)$) using Nd-laser harmonics 2ω and $(3/2)\omega$, respectively.

As shown in Sec. 3, when the thermal conductivity is changed by a factor 30 (f ≈ 0.03) the position of the critical surface changes by only 15-25%, i.e., $R_{cr}(q_{lim}) \sim 0.8R_{cr}(q_{cl})$. The electron-distribution density changes similarly. It is therefore possible to extract

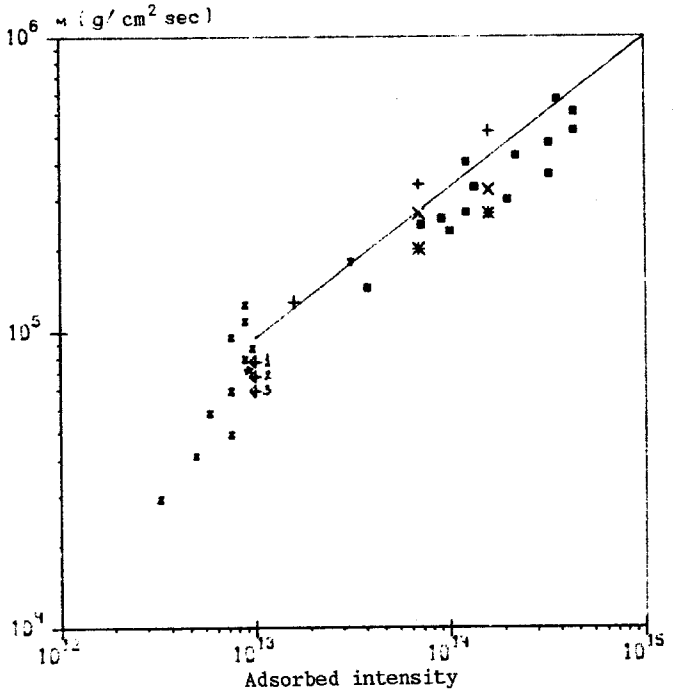

Fig. 6. Dependence of target-mass evaporation rate on the absorbed laser-radiation intensity. Experimental results: ⧗) Rutherford; ■) [31]; *) "KAL'MAR" FIAN. Results of calculation by the "TRITON" program: +) classical heat conduction; ×) model 4, f = 0.03; *) model (5), a = 0.1; solid thin lines) results obtained with stationary corona model; 1) classical heat conduction; 2) f = 0.03; 3) a = 0.03.

from the experiments data on the heat flux only if the experimental data are accurate enough. We analyze next the accuracy of the experimental measurements and determine which of the experimental data permit a reliable assessment of the heat-transfer suppression.

The accuracy of the reduction of the interference patterns is determined by a number of factors. The spatial resolution of the employed optical system (objective–interferometer–photorecorder) is ∿20 μm; the time resolution at a screen scanning rate >2×10^8 cm/sec is not worse than 5×10^{-11} sec [34]. An electron-density error, determined from the interference pattern, is caused also by the procedure of numerically solving the integral equation for the phase advance of the probing radiation. The solution of this incorrectly formulated mathematical problem depends on the character of the sought function and on the method of finding it. Model computations [35] have made it possible to formulate criteria for the optimization of the interferometry procedure. It was shown, in particular, that for a 10% phase-advance mean-statistical measurement error of the phase advance the error in the determination of n does not exceed 10% in a dense laser plasma ($n_e \sim 10^{20}$ cm^{-3}) and 40% on the corona periphery ($n_e < 10^{18}$ cm^{-3} – at the limit of the interferometer sensitivity).

The range of interferometry measurements of the electron density in a laser plasma depends on the wavelength of the probing radiation and on the density gradient near the critical region. Account must also be taken of the refraction of the translucent beams. Refraction prevents the probing beam from reaching the region in which the electron density is of the order of critical. Calculations [34] have shown that in probing at a wavelength λ = 0.532 μm and at the employed objective angular aperture ($2d_f \sim 10^0$) it is possible to record with the "KAL'MAR" facility, under typical experimental conditions, plasma-corona regions of density up to $n_e \sim 3\cdot10^{20}$ cm^{-3}.

It is in fact impossible to process interference patterns at so high a density, even if a sufficiently strong objective is used, because the interference fringes become very crowded. The use of a displacement interferometer [35] has made it possible to measure reliably electron density up to 10^{20} cm^{-3}.

Spectral measurements of $R_{cr}(t)$ and $R_{cr/4}(t)$ (by emission of the 2ω and $(3/2)\omega$ harmonics) yield the indicated values accurate to 10-20 μm. The errors are due in this case to refraction in the inhomogeneous plasma and to the directivity patterns of the 2ω and $(3/2)\omega$ radiation.

5. ANALYTIC ESTIMATES OF THE REQUIRED ACCURACY OF INTERFEROMETRIC DENSITY-PROFILE MEASUREMENTS

As shown in Sec. 4, the laser corona parameters obtained in the computer experiment agree well with the analytic solution for the stationary model of a spherical corona with a spatially variable electronic thermal-conductivity (flux profile (5)). Therefore, based on the latter, we estimate the dependence of the critical radius on the absorbed laser flux q_{abs} and on the degree a of suppression of the heat flux (the factor by which the thermal conductivity is smaller than the Spitzer value).

As follows from [23], R_{cr} is determined by two dimensionless parameter a and γ_0 – in fact a dimensionless combination of the initial data of the problem. For CH targets and for an Nd laser, the second of the above parameters can be written in the form

$$\gamma_c = 8.62 \left(\frac{100\ \mu m}{R_a}\right)^{3/4} \frac{q_{abs}}{10^{13}\ W/cm^2} \tag{7}$$

In the considered "KAL'MAR" experiments [33] ($q_{las} < 10^{14}$ W/cm², $R_a \sim 100$ μm) we have $\gamma_0 < 90$. In the case $0.03 < a < 1$ and $5 < \gamma_0 < 100$ the ratio of the critical and ablation radii can be determined from the following approximate equation [23]:

$$\frac{R_{cr}}{R_a} \approx 1 + 2\mu\left(1 + \sqrt{1 + \frac{\mu}{a}}\right)^{-1} \tag{8}$$

where $\mu = 0.04\ \gamma_0^{3/4} a^{9/16}$.

At a fixed ablation radius, equal changes of the value of R_{cr} can be obtained by changing γ_0 as well as by varying a. The value of γ_0 is proportional to the flux density of the energy (q_{abs}) absorbed in the corona, as calculated from the experimentally measured absorbed energy, and therefore known to within the experimental accuracy. It is therefore possible to draw conclusions concerning the deviation of the heat transfer from the classical value only if the change of the calculated value of R_{cr} as a result of the error Δq_{abs} is less than the change needed to reconcile the theory with experiment.

It follows from (8) that at values

$$\gamma_c \quad > 70\ a^{0.58} \tag{9}$$

the dependence of R_{cr} on energy is weaker than the dependence on a. The condition (9) is well satisfied in KMS FUSION experiments [31] ($q_{abs} = 10^{14}$-10^{15} W/cm², R_a = 50-100 μm). Estimates show that at $\gamma_0 \gg 70\ a^{0.58}$, $R_{cr} - R_a = \Delta R_{cr} \sim q_{abs}^{0.375} a$. The error of q_{abs} has in this case little effect on ΔR_{cr}. Experiment and theory can be reconciled here (see Eq. 3) only by introducing the phenomenological parameter f or a.

With decrease of the flux ($q_{abs} < 10^{14}$ W/cm², $\gamma_0 \lesssim 70\ a^{0.58}$) the dependence of R_{cr} on q_{abs} and on a become approximately equal, and at $q_{abs} \lesssim 10^{13}$ W/cm² the dependence of R_{cr} on q_{abs} is even stronger than on a: $\Delta R_{cr} \sim q_{abs}^{0.75} a^{0.56}$. The character of the $R_{cr}(a)$ dependence has also changed. The position of $R_{cr}(a)$ at $q_{abs} < 10^{14}$ W/cm² depends much more weakly on the degree of suppression of the heat transfer than at higher irradiances ($q_{abs} > 10^{14}$ W/cm²). This imposes more stringent requirements both on the accuracy of the measurement of the position of R_{cr} and on the value of the absorbed energy.

At intensities $q_{abs} \sim 10^{14}$ W/cm² (R_a = 50-100 μm) suppression of the heat transfer by one order of magnitude decreases R_{cr} by 1.5 times. The corresponding 30-60 μm decrease of R_{cr} can be easily recorded by known methods. The same decrease of R_{cr} is obtained in calculations by decreasing flux q_{abs} by 7-10 times. The accuracy of the measured absorbed energy is 20%, so that so strong a change of R_{cr} can be attributed only to heat-transfer suppression, and not to errors in the measurement of the absorbed energy.

At an intensity $q_{abs} \sim 10^{13}$ W/cm^2, for the same target dimensions, suppression of the heat transfer by one order lowers R_{cr} by only 1.1 times ($\sim$15 μm). This change is comparable with the experimental error. Note that the same decrease of R_{cr} could be obtained by decreasing the flux by 3-4 times. This exceeds substantially the experimental error Δq_{abs} and can therefore not be used to explain the observed decrease of R_{cr}.

Consequently, at intensities $q_{abs} < 10^{14}$ W/cm^2 the error in the measurement of the absorbed energy makes a smaller contribution to the calculated $R_{cr}(t)$ dependence compared with the one required to reconcile theory with experiment. To be able to assess in this case the decrease of the thermal conductivity from the position of the critical surface, however, it is necessary to measure $R_{cr}(t)$ with an error <10%.

Since it is difficult in experiment to determine the motion of the critical surface at this accuracy (<10%), it is expedient to determine the heat transfer by comparing the calculated and experimental data on the motion $R_n(t)$ of corona regions with given density $n_e < n_{cr}$. Estimates show that the most reliable information on the heat flux at $q_{abs} < 10^{14}$ W/cm^2 can be obtained by comparing the calculated and experimental $R_n(t)$ for n in the interval $(10^{-2}$-$10^{-1})n_{cr}$.

6. DYNAMICS OF LOW-DENSITY CORONA

The experimental data obtained with the "KAL'MAR" facility and the results of the numerical simulation, by the "TRITON" program, of the motion $R_n(t)$ at densities $n = (10^{-1}, 5\cdot10^{-2}, 10^{-2})n_{cr}$ are compared in Fig. 5.

The target was a CH sphere with initial radius $R_a = 90$ μm and a shell thickness $\Delta R = 2.3$ μm. The Nd-laser pulse had a duration 2.5 nsec and its energy content was $\sim$70 J. The absorbed energy was determined by calorimetry and amounted to 30 J.

We used in the calculations the heat-flux limitation model (4) and various methods of decreasing the electronic thermal conductivity in definite regions, including the model (5). The parameters f and a were varied in the ranges $0.03 \leq f \leq 0.6$, $0.03 \leq a \leq 1$. We determined the values of f and a at which best agreement is obtained between the experimental and calculated dependences.

It was impossible to obtain agreement between experiment and calculation for a flux in the form (5) even when the heat transfer was very strongly suppressed. Calculations with Eq. (5) yield (including also for the classical law a = 1) less compact outer layers of the corona ($n < n_{cr}$) than experiment. Nor is satisfactory agreement obtained by reducing the absorbed energy by one-half, using the classical heat-conduction law in the entire corona (see Fig. 5).

The best agreement between the calculated and experimental $R_n(t)$ dependences was obtained using a heat flux in the form (4) with a restriction f = 0.03. Equal agreement was obtained with the linear form (1) of the flux, in which the thermal conductivity in the entire corona was decreased tenfold compared with the classical value.

This result offers evidence that in the "KAL'MAR" experiments the heat transfer is likewise suppressed by approximately one order and practically in the entire volume of the corona (in contrast to the KMS FUSION experiments, where a good description of the low-density layers of the corona was given by the form (5) corresponding to a decrease of the heat conduction primarily in the region between the ablational and critical surfaces).

7. EVAPORATION RATE $\dot{m}$

Figure 6 shows the measured $\dot{m}$ in various experiments with spherical targets, as functions of the energy flux density absorbed in the corona. The same figure shows the values of $\dot{m}$ calculated for a stationary model of the corona [23] and by the "TRITON" program, both for the parameters of the KMS FUSION experiments (see Sec. 3) and in the experiments on the "KAL'MAR" facility.

We note first that the change of $\dot{m}$ with allowance made in the calculation for the lowered heat conduction (f = 0.03 or a $\approx$ 0.03) is different for different absorbed-energy values. At intensities $q_{abs} \approx 10^{13}$ W/cm^2 lowering the thermal conductivity in the calculation by the "TRITON" program to one-thirtieth of the classical value decreases m by only 1.3 times. The same lowering of the heat conduction for $q_{abs} \approx 10^{14}$ W/cm^2 decreases $\dot{m}$ by a factor 2.5.

Similar estimates follow also from the stationary model of the corona [23], according to which an intensity change from 10^{13} to 10^{14}-10^{15} W/cm^2 causes a change from $\dot{m} \sim a^{1/8}$ to $\dot{m}^* \sim a^{1/4}$.

Thus, for low fluxes ($q_{abs} < 10^{13}$ W/cm^2) suppression of heat transfer influences little the mass evaporation rate. Experimental (including those obtained with the "KAL'MAR" facility) and calculated data on $\dot{m}$ agree well (within the limits of experimental error) when the heat conduction is decreased by approximately one order; the need for introducing the decrease follows from a comparison of the experimental and calculated $R_{cr}(t)$ dependences.

For $q_{abs} > 10^{14}$ W/cm^2 the data on $\dot{m}$ and $R_{cr}(t)$ (calculated and experimental) can be reconciled only by lowering the thermal conductivity by 10-30 times.

8. CONCLUSION

From the foregoing analysis we can draw the following conclusions:

1. Lowering the heat conduction leads first of all to a change of the geometric dimensions of the corona. The most reliable information on the heat fluxes can thus be obtained by analyzing the spatial and temporal evolutions of the electron-density distribution.

2. Interferometry measurements of the density profile in the corona and measurements of the fraction of absorbed energy reveal, in experiments at intensities $q_{abs} > 10^{13}$ W/cm^2, a decrease of the heat conduction by more than an order compared with the classical value.

3. The aggregate of the experimental data obtained with the "KAL'MAR" facility at $q_{abs} < 10^{14}$ W/cm^2 cannot be described by calculation using the classical heat-conduction law. Inteferometry data on the dynamics of a low-density corona can be reconciled with a numerical calculation of the trajectories of the densities $n = (10^{-2}$-$10^{-1})n_{cr}$ either by introducing the limitation (2) with f = 0.03 or by suppressing the heat conduction in the entire corona by approximately one order.

LITERATURE CITED

1. L. Spitzer and R. Harm, "Transport phenomena in a completely ionized gas," Phys. Rev., 89, 977-881 (1957).
2. L. Spitzer, Physics of Fully Ionized Gases, Wiley (1962).
3. B. Yaakobi and T. C. Bristow, "Measurement of reduced thermal conduction in (layered) laser-target experiments," Phys. Rev. Lett., 38(7), 350-353 (1977).
4. M. S. White, J. D. Kilkenny, and A. E. Dangor, "Measurement of thermal conductivity in a laser-heated plasma," Phys. Rev. Lett., 35(8) (1975).
5. F. Amiranoff, R. Fabbro, E. Fabre, C. Garban, J. Virmont, and M. Weinfeld, "Experimental transport studies in laser-produced plasmas at 1.06 and 0.53 μm," Phys. Rev. Lett., 43(7), 522-525 (1979).
6. M. D. Rosen, D. W. Phillion, V. S. Rupert, et al., "The interaction of 1.06-μm laser radiation with high Z disk targets," Phys. Fluids, 22(10), 2020-2031 (1979).
7. W. Yaakobi, J. Delettrez, L. M. Goldman, R. L. McCrory, R. Marjoribanks, M. C. Richardson, D. Shvarts, S. Skupsky, J. M. Soures, S. Verdon, and D. M. Villeneuve, "Thermal transport measurements in 1.05 μm laser irradiation of spherical targets," Phys. Fluids, 27(2), 516-526 (1984).
8. G. H. McCall, "Laser-driven implosion experiments," Plasma Phys., 25(3), 237-285 (1983).
9. L. L. Cowie and C. F. McKee, "The evaporation of spherical clouds in a hot gas. 1. Classical and saturated mass loss rates," Astrophy. J., 211, 135-146 (1977).
10. C. E. Max, W. M. Manheimer, and J. J. Thomson, "Enhanced transport across laser-generated magnetic fields," Phys. Fluids, 21(1), 128-139 (1978).
11. M. Strauss, G. Harak, D. Shvarts, and R. S. Grahton, "Magnetic field effects on electron heat transport in laser-produced plasmas," Phys. Rev. A: Gen. Phys., 30(5), 2627-2637 (1984).
12. E. M. Epperlein and M. G. Haines, "Plasma transport coefficients in a magnetic field by direct numerical solution of the Fokker–Planck equation," Phys. Fluids, 29(4), 1029-1041 (1986).
13. R. J. Bickerton, "Thermal conduction limitation in laser fusion," Nucl. Fusion, 13, 457-458 (1973).
14. I. B. Bernstein, C. E. Max, and J. J. Thomson, "Effects of high-frequency fields on plasma transport coefficients," Lawrence Livermore Laboratory, Preprint UCRL-80335, November 9, 1977.

15. D. R. Gray and J. D. Kilkenny, "The measurement of ion acoustic turbulence and reduced thermal conductivity caused by a large temperature gradient in a laser heated plasma," Plasma Phys., 22, 81-111 (1980).
16. P. Manchicourt and P. A. Holstein, "Heat flux limitation by ion-acoustic instability," Phys. Fluids, 23(7), 1475-1476 (1980).
17. C. E. Max, C. F. McKee, and W. C. Mead, "A model for laser driven ablative implosions," Phys. Fluids, 23(8), 1620-1645 (1980).
18. A. R. Bell, R. G. Evans, and D. J. Nicholas, "Electron energy transport in steep temperature gradients in laser produced plasmas," Phys. Rev. Lett., 46, and 243-246 (1981).
19. J. F. Lusiani, P. Mora, and R. Pellat, "Quasistatic heat front and delocalized heat flux," Phys. Fluids, 28(3), 835-845 (1985).
20. P. P. Volosevich, V. I. Kosarev, and E. I. Levanov. "Allowance for confinement of heat flux in a computer experiment," Preprint 21, Inst. Appl. Mech. USSR Acad. Sci. (1978) [in Russian].
21. G. B. Zimmerman, "Numerical simualtion of the high density approach to laser-fusion," Lawrence Livermore Laboratory, Preprint UCRL-74811 (1977), p. 47.
22. J. P. Cristiansen, D. E. T. F. Ashby, and K. V. Roberts, "MEDUSA: A one-dimensional laser fusion code," Comp. Phys. Commun., 7(5), 271-278 (1974).
23. E. G. Gamalii, A. E. Kiselev, "Effect of spatially varying coefficient of electronic heat conduction on the characteristics of a laser corona," Preprint 122, FIAN USSR (1986).
24. M. D. Rosen, "Evidence of a laser intensity threshold for the onset of inhibited electron transport," Comments Plasma Phys. Controlled Fusion, 8(5), 165-175 (1989).
25. Yu. V. Afanas'ev, N. G. Basov, B. L. Vasin, et al., "Investigation of physical processes in the corona of laser irradiated shell targets," Zh. Éksp. Teor. Fiz., 77(6), 2539-2554 (1979).
26. N. G. Basov, S. I. Chebotarev, A. E. Danilov et al., "Measurement of the dynamics of the compression of high-aspect-ratio shell targets in the 'DELFIN-1' installation," Phys. Lett., 105a(8), 410-414 (1984).
27. P. P. Volosevich, N. A. Dar'in, G. A. Evseev, et al., "Simulation of mass and energy transport in a program for solving high-temperature-plasma problems," in: 10th All-Union School of Theoretical and Applied Problems of Computational Mathematics and Mathematical Physics, Riga, Latv. State Univ. (1985), pp. 171-172.
28. A. A. Samarskii, S. A. Gaifullin, A. V. Zakharov, et al., "DIANA program for calculating one-dimensional problems in laser-driven thermonuclear fusion," VANT, Ser. Metodiki i Programmy (1983), No. 2(13), pp. 38-42.
29. E. G. Gamalii, A. E. Kiselev, E. I. Levanov, S. E. Osokin, and E. I. Sotskii, "Phenomenological models of electronic heat conduction," in: All-Union School-Seminar "Mathematical Simulation in Science and Engineering," Perm. (1986), pp. 86-87.
30. J. A. Tarvin, W. B. Fechner, J. T. Larsen, P. D. Rockett, and D. C. Slater, "Mass-ablation rates in a spherical laser-produced plasma," Phys. Rev. Lett., 51(15), 1355-1358 (1983).
31. W. W. Fechner, C. L. Shepard, Gar. E. Busch, R. J. Schroeder, and J. A. Tarvin, "Analysis of plasma density profiles and thermal transport in laser-irradiated spherical targets," Phys. Fluids, 27(6), 1552-1560 (1984).
32. Yu. V. Afanas'ev, E. G. Gamalii, O. N. Krokhin, and V. B. Rozanov, "Stationary model of corona of spherical laser targets," Zh. Éksp. Teor. Fiz., 71(2), 594-602 (1976).
33. N. G. Basov, Yu. A. Zakharenkov, N. N. Zorev, G. V. Sklizkov, A. A. Rupasov, and A. S. Shikanov, "Heating and ablation of laser-irradiated thermonuclear targets," in: Itogi Nauki i Tekh., Ser. Radiotekh., 26, No. 2 (1982), p. 47.
34. A. A. Erokhin, Yu. A. Zakharenkov, N. N. Zorev, et al., "Methods of optical probing of inhomogeneous plasma," Trudy FIAN, 149, Nauka, Moscow (1985), pp. 97-124.
35. Yu. A. Zakharenkov, G. V. Sklizkov, and A. S. Shikanov, "Use of displacement-interferometry for diagonostics of dense inhomogeneous plasma," Fiz. Plazmy, 6(2), 453-462 (1980).